Computer Science Review 35 (2020) 100203

Contents lists available at ScienceDirect

Computer Science Review

journal homepage: www.elsevier.com/locate/cosrev

Review article

Application of deep learning for retinal image analysis: A review

Maryam Badar [a], Muhammad Haris [a,*], Anam Fatima [b]

[a] School of Electrical Engineering and Computer Science, National University of Sciences and Technology, Islamabad, Pakistan
[b] University of Engineering and Technology, Lahore, Pakistan

ARTICLE INFO

Article history:
Received 13 May 2019
Received in revised form 14 September 2019
Accepted 4 November 2019
Available online 18 December 2019

Keywords:
Deep learning
Deep neural network
Convolutional neural network
Auto-encoder
Sparse stacked auto-encoder
De-noised sparse auto-encoder
Softmax
Random forest
Rectified linear unit
Hidden layers

ABSTRACT

Retinal image analysis holds an imperative position for the identification and classification of retinal diseases such as Diabetic Retinopathy (DR), Age Related Macular Degeneration (AMD), Macular Bunker, Retinoblastoma, Retinal Detachment, and Retinitis Pigmentosa. Automated identification of retinal diseases is a big step towards early diagnosis and prevention of exacerbation of the disease. A number of state-of-the-art methods have been developed in the past that helped in the automatic segmentation and identification of retinal landmarks and pathologies. However, the current unprecedented advancements in deep learning and modern imaging modalities in ophthalmology have opened a whole new arena for researchers. This paper is a review of deep learning techniques applied to 2-D fundus and 3-D Optical Coherence Tomography (OCT) retinal images for automated classification of retinal landmarks, pathology, and disease classification. The methodologies are analyzed in terms of sensitivity, specificity, Area under ROC curve, accuracy, and F score on publicly available datasets which includes DRIVE, STARE, CHASE_DB1, DRiDB, NIH AREDS, ARIA, MESSIDOR-2, E-OPTHA, EyePACS-1 DIARETDB and OCT image datasets.

Contents

* Corresponding author.
E-mail address: mharis.msit15seecs@seecs.edu.pk (M. Haris).

https://doi.org/10.1016/j.cosrev.2019.100203
1574-0137/

1. Introduction

Automatic classification of ophthalmologic and cardiovascular diseases through analysis of retinal images has become an established practice in telemedicine. Earlier techniques involved manual segmentation but it was monotonous, time-consuming, inconvenient, labor intensive, observer driven, and required proficient skill [1] whereas computer-aided detection of retinal abnormalities is cost-effective, feasible, objective, and does not require efficiently trained clinicians to grade the images [2]. Development of screening systems are helpful in early diagnosis and real time classification of retinal diseases such as Diabetic Retinopathy (DR), Age Related Macular Degeneration (AMD), Macular Bunker, Retinoblastoma, Retinal Detachment, and Retinitis Pigmentosa [3]. A number of template, edge, and morphology based algorithms have been presented in the past for auto delineation of retinal landmarks and retinal pathology [4,5]. Moreover, several supervised and unsupervised neural networks based methods have also been employed for retinal image analysis. Many supervised methodologies adopted SVM, MLP, ANN and decision trees [6–8]. Similarly, matched filtering and model based approaches have been scrutinized for the purpose of unsupervised retinal abnormality detection [9].

All these state-of-the-art methods required manual feature designing through SURF, SIFT, and HOG feature descriptors [10–12]. The explicit domain knowledge is mandatory requirement for this kind of hand crafted feature extraction. Most of the times the results obtained through them are more specialized on a dataset and generalization is not achieved. Recent advancements in visual recognition via deep learning have invigorated researchers to employ these techniques in the field of ophthalmology as well. Automatic learning of intricate features in the retinal images can be obtained by the use of deep learning. The supervised and unsupervised multi-layer Deep Neural Networks (DNN) allow generalized high level feature extraction from raw data image. Whereas, retinal image analysis based on deep learning has outperformed the traditional methods both for 2-D fundus images and 3-D Optical Coherence Tomography (OCT) images.

Abràmoff et al., have discussed retinal imaging and retinal image analysis based on 2-D fundus and 3-D OCT images. However, this review encompasses only conventional techniques for retinal deformity detection. Moreover there are many other reviews and survey papers which cover the domains of retinal landmark detection, retinal pathology segmentation, and retinal disease classification [1,13]. The major contribution of this paper lies in the fact that there is no existing survey paper which covers deep learning based retinal image analysis. This work is a review of 2-D fundus and 3-D OCT retinal images' analysis using modern deep learning techniques for automated identification of retinal landmarks, pathology, and disease classification. We have analyzed and compared algorithms on the basis of a diverse set of performance metrics which include: sensitivity, specificity, area under ROC curve, and accuracy. The objective of this work is to summarize the current progress made in the field of ophthalmology using deep learning techniques.

1.1. Methodology of literature search

A systematic methodology has been developed for searching literature for this study. This systematic methodology includes the following stages:

- Defining research problem
- Finding pertinent articles that satisfy the pre-set inclusion criteria
- Extracting relevant data from articles
- Assessment of quality of extracted data

All the literature that has been reviewed in this survey was retrieved by conducting iterative and exhaustive searches on following databases:

1. IEEE Xplore Digital Library, (http://ieeexplore.ieee.org)
2. Springer Link, (http://link.springer.com/)
3. ScienceDirect, (http://www.sciencedirect.com/)
4. American academy of Ophthalmology, (http://www.aaojournal.org/)
5. The JAMA Network, (http://jamanetwork.com/journals/jama)
6. Investigative Ophthalmology and Visual Science, (http://iovs.arvojournals.org/)

All journal papers as well as conference papers that have been published in the proceeding of above mentioned bibliographic databases have been included in this review. Keywords that have been used to perform the search are: deep learning, deep neural network (DNN), convolutional neural network (CNN), auto-encoder, stacked sparse auto-encoder (SSAE), denoised sparse auto-encoder (SDAE), softmax, random forest, rectified linear unit, hidden layers, DR, exudate detection/ segmentation, microaneurysms detection/segmentation, Optic Disc (OD) localization, fovea localization, retinal blood vessel segmentation, AMD, automated screening, retinal disease classification.

1.2. Inclusion criteria

"Application of deep learning for retinal image analysis" has been set as the cue statement for literature search. Abstracts and titles of all collected articles are checked against the research cue and only those articles are selected which provide deep learning based algorithms for segmentation of retinal anatomical structures and retinal disease classification. All the relevant content up till December, 2018 has been included in this survey.

1.3. Exclusion criteria

The main focus of this survey is to review deep learning based techniques for retinal image analysis. Therefore, the articles whose algorithms are not based on deep learning concepts are excluded from this survey. Moreover, the articles from impact factor journals and reputed conferences have been selected in this review. We have avoided inclusion of such papers which were published in local journals and conferences.

1.4. Selection of papers

Articles were selected through vigilant scrutiny of inclusion and exclusion criteria. Selected articles were downloaded in pdf format and saved. The nomenclature used for saving selected papers depict publishing year, journal name/conference name, publisher, main author name, and title. This type of nomenclature helped in indexing the articles and resulted in efficient retrieval in accordance with queries. Citations of all the articles have also been downloaded and saved in EndNote library.

2. Diagnostic analysis and screening of retinal images

2.1. Retinal imaging modalities

Precise imaging of retinal tissues and brain tissues is very important for the diagnosis and treatment of retinal impairments. Czech scientist Jan Evangelista Purkyně [14] invented principles of ophthalmoscope in 1823 as a first attempt towards direct inspection of retina. Since then many imaging modalities have been developed for non-destructive visualization of retinal anatomical structures. Fundus photography has been found to be effective for early screening and diagnosis of three most important causes of blindness in industrialized world i.e. macular degeneration, glaucoma, and DR. The 2-D representation of retinal world obtained by preliminary fundus cameras lacked the ability to apprehend depth during examination of fundus image which lead to inaccurate diagnosis of certain retinal pathology (e.g. cotton wool spots). Tomography based imaging has resolved this problem. OCT has now been successfully employed to develop 3-D view of retina [15].

2.1.1. Fundus photography

The process of obtaining a 2-D representation of 3-D ocular fundus through projection of reflected light on to an imaging plane is termed as fundus photography. Fundus photography, mydriatic or non mydriatic, involves use of a low power intricate microscope with an attached camera for imaging the interior surface of the eye which includes retina, OD, retinal vasculature, posterior pole, and macula. Digital Imaging of inner lining of eye surface through fundus photography follows the same footings as those of conventional image capturing except that instead of a photographic film, digital cameras have sensors (charge coupled device or complementary metal oxide semiconductor active pixel). Each sensor converts light signal into electric signal and result is stored in the form of a single pixel. The resolution of image can be increased by increasing number of sensors.

Advancements in the models of fundus photography have been witnessed since the last century [2]. The modern fundus photography includes the following imaging modalities:

Color fundus photography modifies spectral range of illumination source through the use of contrast filters (red, blue, and green filters). This variability in spectral range of illuminating source enhances visibility of several ocular structures. For instance, blue color improves perceptibility of anterior retinal layers, which appear transparent in the presence of white light. Moreover, blood vessels and retinal pigments absorb blue light resulting in a dark background which enhances specular reflections and scattering in anterior fundus layers. On the other hand, green light provides the best global retinal view because the retinal pigmentations reflect green light more than blue light providing excellent contrast. Hence, green filter is employed in color fundus photography for improved visualization of retinal vasculature, drusen, exudates, and hemorrhages. Retinal pigments, blood vessels and optic nerve appear almost featureless in red light and overall contrast of retinal images is reduced. Hence, red light is only used for revealing the choroidal pattern, pigmentary disturbances, choroidal ruptures, choroidal naevi, and choroidal melanomas [16].

Red free photography is the process of retinal image acquisition in the presence of an illumination source with a specific color filter to block red light, usually green filter is used for this purpose. This kind of fundus photography is effective in viewing retinal blood vessels, hemorrhages, pale lesions (exudates and drusen), epiretinal membranes, and retinal nerve fiber layer defects [17].

Stereo fundus photography [18] helps in documenting the retinal structures because of its increased depth resolution feature. This type of photography involves simultaneous or sequential visualization of retina through two cameras with different angles of observation insuring least stress to the patient and it is viable for diagnosis of macular edema (ME) and sub retinal neovascularization.

Hyper-spectral imaging allows efficient visualization of retinal lesions with high spatial and spectral resolution. The illumination source has multiple wavelength bands and their reflection is recorded in the form of hyper-spectral image intensities. This type of imaging modality is feasible for retinal blood oxygen saturation analysis (oximetry) [19] through likening of spectral absorptions by retinal arteries, veins, and surrounding regions. Hyper-spectral imaging is appropriate for screening and diagnosis of diseases such as: diabetes, AMD, and glaucoma [20].

Scanning Laser Ophthalmoscopy (SLO) [21] uses a focused laser beam to illuminate the retinal fundus and provides retinal images with high spatial sensitivity. It is helpful in diagnosis of retinal disorders such as macular degeneration and glaucoma.

Adaptive Optics SLO [22] utilizes SLO and enhances the results by removing aberrations from retinal images through adaptive optics. The retinal images obtained by adaptive SLO are sharper than those obtained by SLO.

Angiography is the process of injecting fluorescent dye in retinal blood vessels and projection of emitted photons from the dye on to an imaging plane. The fluorescent dye, which is injected in circulation, is sensitive to the light reaching it i.e. the fluorescence is different for different wavelengths of light. This chameleon behavior of fluorescent dye makes angiography an apposite imaging modality for inspection of retinal blood circulation [23].

1. ***Sodium Fluorescein Angiography (FAG)*** is a variation of angiography. However, the fluorescent dye injected in retinal blood circulation is sodium. When the retinal blood vessels and neighboring retinal tissues are illuminated with blue light (490 nm wavelength), the dye fluoresces yellow light (530 nm wavelength). It is helpful in documenting the retinal manifestaions of cystoid macular edema and DR [23].
2. ***Indocyanine Green Angiography (ICG)*** is another variant of angiography which employs indocyanine as fluorescence agent. The injected indocyanine glows only in infrared spectrum thereby making the blood, fluids, and choroidal pigments, present in posterior part of eye, transparent for the observer. This behavior makes it appropriate

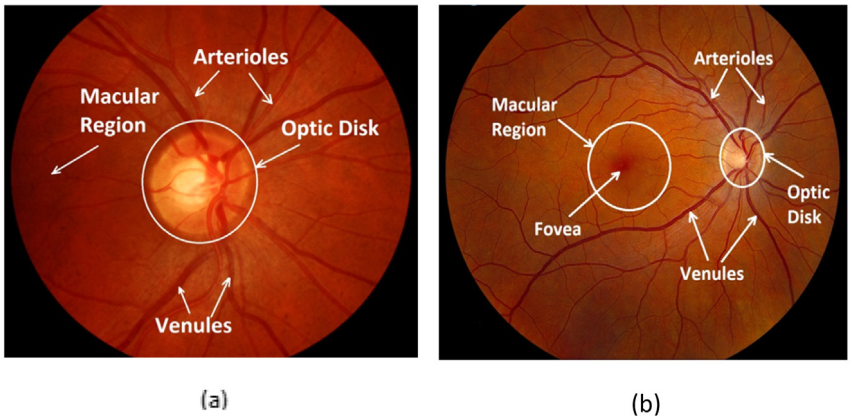

Fig. 1. Retinal fundus images (a) OD centered (b) Macula centered.

for diagnostic analysis of deep choroidal disorders such as choroidal neovascularization, abnormal vessels supplying ocular tumors, and hyperpermeable vessels leading to central serous chorioretinopathy [24].

A diverse set of datasets based on retinal fundus photography, from different ethnicities, has been developed. Some of them are publicly available while others can be obtained on demand. A brief overview of these datasets is presented in Table 1.

2.1.2. 3-D optical coherence tomography (OCT)

OCT [25] is a widely accepted noninvasive imaging modality among ophthalmologists. This technique captures 3-D cross-sectional maps of retina by utilizing the principle of interferometry and confocal microscopy. Accuracy of 3-D OCT images is usually 10 to 15 μm. Depending on the light source used, resolution of images can be improved. The illumination source with large wavelength is preferable because it provides efficient scattering of light in retinal cross-section. These images are efficient in diagnosis of macular pucker, vitreomacular traction, macular hole. However, OCT has recently been regarded as a new standard for detection of diabetic macular edema. The advancement in technologies has made OCT capable of generating angiograms for assessment of retinal vasculature.

2.2. Retinal anatomical structures

Human eye, which is mostly a hollow organ, is internally lined by light sensitive tissues collectively named as the retina. The posterior pole of the eye is tightly knit with neuronal cells, photoreceptor cells, and glial cell. Rods, cones and ganglion cells are three types of photoreceptor cells. The optic nerve fibers originate from nerve fiber layers which emanate from axons of ganglion cells. The ocular structures focus the image on retina and nerve fibers transfer the information to brain in the form of electrical signals which then interprets the received signals as visual images. Optic nerve head or OD, oval in shape, serves as the exit point for nerve fibers and is located 4.5 mm to 5 mm nasal to the center of retina as depicted in Fig. 1. The maximum resolving power of the eye comes from the anatomical center of eye i.e. macula. Fovea and foveola are resent in the macular region and both of them contain a large number of photoreceptors (cones) making them specialized retinal region for high acuity vision [26]. Visual capacity of human brain is primarily dependent on visual input from macula but progressive damage to macula results in inculcation of diseases like macular degeneration or in severe cases can create macular hole bursting the blood vessels coursing towards macula.

Ophthalmic artery provides the circulation to the retina. Retinal blood vessels exist in the form a network of arterioles and venules which circulate the whole retinal region. Due to nonfenestration of the vascular endothelium a blood–retina barrier is maintained by retinal blood vessels. Microaneurysms and hemorrhages are produced as a result of damage to this blood–retinal barrier. Moreover, out pouching of retinal blood vessels appear as neovascularization disturbing their morphology. Various systemic and retinal diseases manifest themselves in the form of variation in retinal blood vessels' features.

2.3. Disease manifestations as retinal impairments

Analysis of retinal morphology provides an insight to general health state of entire human body as many systemic and retinal diseases manifest themselves as ocular structures' impairments. Following rubrics provide a compact overview of such diseases.

2.3.1. Diabetic retinopathy (DR)

Diabetes mellitus (DM) is a disease caused by fluctuating levels of glycemia (hypoglycemia, hyperglycemia). Repercussions of DM can emanate as asymptomatic development of DR (damage to the eyes), diabetic nephropathy (damage to kidneys), and diabetic neuropathy (damage to nerve) [27]. The most prevalent consequence of DM is DR. Despite the use of intensive glycemic control therapy DR remains a vision threatening complication of diabetes. Severe symptoms of DR include development of microaneurysms, neovascularization, hemorrhages, cotton wool spots, and exudates in the retinal region. Extreme progression of polygenic disease puts the patient's eyesight at stake [28]. Pathogenesis like capillary closure and dysfunction of blood–retina barrier are the main anatomical changes in retina that lead to DR. Their brief detail is mention in the following sections.

2.3.1.1. Retinal vessel closure. Many retinal disorders stem from obliteration of retinal capillaries such as neovascularization is reported to be preceded by nonperfusion and closure of small retinal blood vessels [29]. Retinal vessel closure instigates the development of neovascularization, microaneurysms, cotton wool spots, and hemorrhages.

Neovascularization Retinal blood vessel closure leads to limited supply of oxygen to retinal regions corresponding to these vessels. This condition is often termed as retinal ischemia [30]. The vascular endothelial growth tries to compensate the decreased oxygen supply resulting in the formation of weak small blood vessels on the surface of retina thereby leading to vision loss.

Microaneurysms: Limited oxygen supply results in unusual dilation of retinal capillaries. These bulgings of capillary endothelial

Table 1
Specifications of 2-D fundus Retinal Image Datasets.

Sr.	Dataset	Source	Camera Specs.	Field of view (FOV)	Image format	Image size (pixels)	Number of Images	Ground Truth	Availability
1	DRIVE [31]	DR screening test held in Netherlands	Canon CR5 non-mydriatic 3-CCD camera	45°	JPEG compressed	768× 584	40	Blood Vessel demarcation	Public
2	STARE [32]	Shiley Eye Center at the University of California, San Diego, Veterans Administration Medical Center in San Diego.	TopCon TRV-50 fundus camera	35°	–	605x 700	20	Blood Vessel demarcation	Public
3	ARIA [33]	St. Paul's Eye Unit, Royal Liverpool University Hospital Trust, Liverpool, UK and the Department of Ophthalmology, Clinical Sciences, University of Liverpool, Liverpool, UK	Zeiss FF450+ fundus camera	50°	Uncom-pressed TIFF	768x 576	212	Trace of blood vessels, the optic disc and fovea location	Public
4	CHASE_DB1 [6]	Child Heart and Health Study in England (CHASE), a cardiovascular health survey in 200 primary schools in London, Birmingham, and Leicester	Nidek NM-200-D	30°	TIFF	1280x 960	28	Blood Vessel demarcation	Public
5	DIARETDB0 [34]	Captured under IMAGERET project	Several digital fundus cameras	50°	PNG	1500x 1152	130	Each image is marked as having any red small dots, hemorrhages, hard exudates, soft exudates, neovascularization or not	Public
6	DIARETDB1 [35]	Captured under IMAGERET project	Several digital fundus cameras	50°	PNG	1500x 1152	89	Demarcation of red small dots, hemorrhages, hard exudates, and soft exudates	Public
7	MESSIDOR-2 [36]	LaTIM laboratory and the Messidor program partners	TopCon TR NW 6 3CCD fundus camera	45°	TIFF	1440 x 960 2240 x 1488 2304 x 1536	1748		On demand
8	E-Ophtha EX [36]	ANR-TECSAN-TELEOPHTA project	-	-	JPEG	2544x 1696 2048x 130 1440x 960	82	Exudates marked	Public
	E-Ophtha MA [36]	ANR-TECSAN-TELEOPHTA project	-	-	JPEG	2544x 169 1440x 960	381	Microaneurysms marked	Public
9	NIH AREDS	Project funded by NIH	–	–			5600		Public
10	DriDB [37]	university hospital in Zagreb	Zeiss VISUCAM 200 fundus camera	45°	Uncom-pressed BMP	720x 576	50	location of OD, blood vessels, hard exudates, soft exudates, dot and blot hemorrhages, and neovascularization	On Demand
11	EYE-PACS1	Captured during regular screening of DR affected patients under EYEPACS program	Canon CR1/DGi/CR2, Centervue DRS, and Topcon NW camera	45°	JPEG	Varying sizes	9963	Each image marked as having: No DR, Mild, Moderate, Severe or Proliferative DR	Public

linings often appear in the form of small sac like structures named as microaneurysms. The fragility of capillary walls is considered to be the main reason behind development of microaneurysms [38]. They appear as small red dots in retinal images as depicted in Fig. 2.

Cotton wool spots: Oxygen supply to certain retinal areas may completely close off due to blockage in arterioles. Consequently large regions of retina become completely deprived of oxygen and result in emanation of fluffy white patches identified as cotton wool spots or soft exudates [38].

Hemorrhages: The blockade in arterioles may instigate a pressure build up within the vessels. Significant amount of pressure could burst the vessels and result in origination of hemorrhages [38] as shown in Fig. 2.

2.3.1.2. Mutilation of blood–retina barrier. Retinal blood vessels are permeable i.e. they allow motion of fluids through their walls. In DR, the retinal vessels become fenestrated and abnormal leakage of blood cells, proteins, water and other large molecules starts.

Hard Exudates: They appear as a consequence of leakage of fats and proteins along with water from abnormally permeable walls of retinal vessels. Mostly hard exudates appear on the outer layer of retina individually, in the form of patches, or surrounding microaneurysms in the form of a crescent. They appear as yellowish, waxy, and glistering structures in retinal images as presented in Fig. 2.

2.3.1.3. Macular edema. The central region of retina is macular region and is responsible for high acuity vision. Macular edema (ME) is a consequence of retinal thickening near macula and fenestration of retinal blood vessels. The anomalous vasopermeability allows abnormal flow of large molecules like water, blood cells, lipids, and proteins through retinal vascular walls. Accumulation of such fluids in the macular region results in the development of pigments such as exudates leading to ME. Treatment of ME is only recommended when the pigmentations develop at the center of macula i.e. fovea. This condition is termed as clinically significant macular edema (CSME). CSME is actually defined as presence of hard exudates within 500 μm of the macular or retinal thickening within 500 μm of the macular region [39]. Prolonged and asymptotic DM results in the origination of diabetic macular edema preceded by proliferative and non-proliferative DR [40].

Severity levels of DR have been graded based on the variants of pathology present in retina. A brief detail about grading levels of DR, in accordance with the severity, is presented below:

Proliferative DR (PDR) is marked by presence of retinal hemorrhages.

Moderate PDR manifests itself in the form of neovascularization and retinal hemorrhages.

Severe PDR is indicated by the presence of detachment of retina and neovascularization on iris.

Insignificant non-proliferative PDR (NPDR) signs are microaneurysms, retinal hemorrhages, and hard exudates

Significant NPDR has similar signs as those of insignificant NPDR with vessel closure.

High Risk NPDR depicts itself as retinal hemorrhages and vessel closure.

Moderate ME is indicated by hard exudates, origination of Edema outside fovea region, and thickening of retina.

Severe ME manifestations are similar as those of moderate ME except that Edema develops inside the fovea region.

2.3.2. Age related macular degeneration (AMD)

For people of age above 50 years, AMD is found to be the chief cause of irreversible vision loss. Presence of AMD is characterized by excessive presence of drusen, yellow dots, in the macular region of eye. Small number of hard drusen is not regarded as symptoms of AMD because people with age more than 50 years are likely to develop drusens as a normal anatomy of retina. But anomalously large number of drusen can result in mutilation of retinal pigment epithelium [41]. AMD can be classified into the following categories:

Early AMD is marked by the presence of less than 20 medium sized drusen or other abnormal retinal pigments [42].

Intermediate AMD is characterized by the presence of many medium sized drusen, one large druse or geographic atrophy that is away from the center of macula [42].

Advanced non-neovascular AMD (Dry AMD) manifests itself in the form of drusen and geographic atrophy that extends to fovea i.e. the center of macula [42].

Advanced neovascular AMD (Wet AMD) is indicated by presence of exudates, neovascularization, and sequelae of neovascularization [42] (see Fig. 3).

2.3.3. Cardiovascular diseases

Coronary heart disease is directly linked with micro-vascular circulation. Changes in microvasculature, structure and pathology of human circulation can be studied through in vivo examination of retina. Therefore, retinal image analysis provides a window in the health of human heart. Common retinal vascular signs include formation of microaneurysms, hemorrhages, arterio-venous nicking, and focal arteriolar narrowing. These signs reflect vascular damage because of hypertension, aging, and other processes. Retinal vascular narrowing is found to be associated with reduced myocardial perfusion measures on cardiac magnetic resonance imaging. Moreover, it has also been found that other retinopathy lesions are linked to coronary artery calcification. These kind of anatomical and pathological reasons suggest that changes in retinal microvasculature can be useful for assessing the coronary heart disease risk stratification [43].

2.3.4. Glaucoma

The second most prevalent cause of permanent vision loss in the developed world is glaucoma. This disease directly damages the optic nerve and the ganglion cells [44]. Optic nerve of glaucoma affected eye shows cupping of optic nerve up to an abnormal amount. Obesity, high blood pressure, migraines, and increased pressure in eye are the factors that instigate glaucoma. Glaucoma is classified as open angle, close angle, and normal tension glaucoma. Open angle glaucoma is the most prevalent type of glaucoma. It grows gradually and is painless but it has the potential of making the patient completely blind if left untreated. However, closed angle glaucoma has the ability to manifest itself slowly or abruptly. Normal tension glaucoma is associated with blood circulation issues in retinal area and other organ perfusion whereas the classic hallmark of intra-occular pressure has no association with this kind of glaucoma. Glaucoma is diagnosed by analysis of intra-ocular pressure, cup to disk ratio, retinal vascular morphology, optic nerve structure, and anterior chamber angle [45].

2.4. Quantitative measures for retinal image analysis

An algorithm is considered efficient if its predictions and ground truth stand in close proximity to each other. This proximity can only be tested by the use of some quantitative measures. These quantitative measures also help in evaluating and comparing the capabilities of different algorithms. Sophisticated performance metrics are derived from basic performance measures

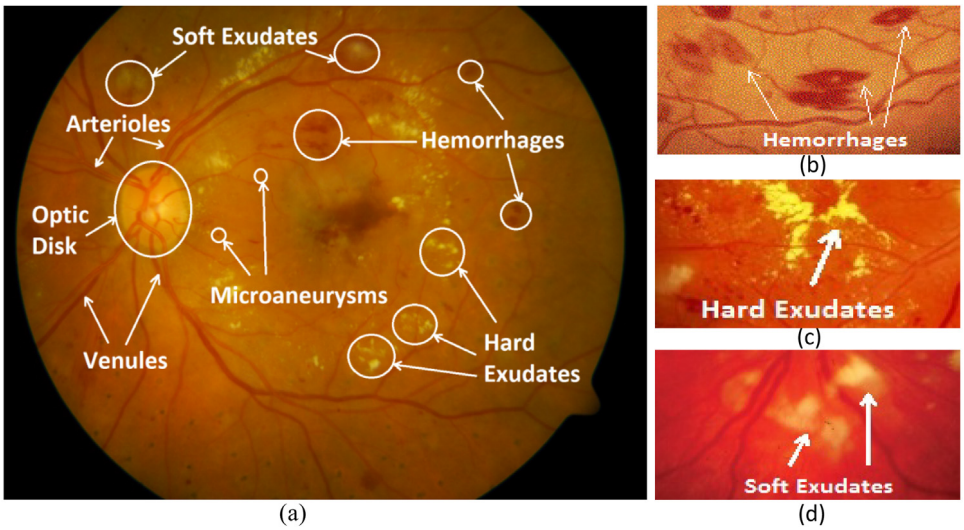

Fig. 2. (a) Retinal image with pathologies (b) Hemorrhages (c) Soft Exudates (d) Hard Exudates.

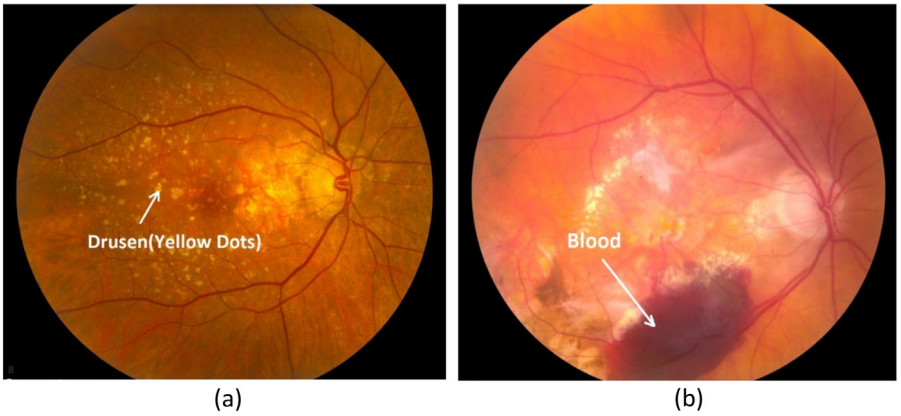

Fig. 3. Retinal image diagnosed (a) with Dry AMD (b) with Wet AMD.

(true positives, false positives, true negatives, and false negatives). The performance metrics which are used for analysis and comparison of algorithms in this study are recorded in Table 2.

Ratio of classified exudate pixels to the total pixels plus ratio of pixels classified as non-exudates to the total pixels.

3. Deep-learning

Creation of self-taught and self-thinking machines has remained utter desire of humans since antiquity. With the invention of programmable computers, scientists remained focused towards tackling problems which were intellectually difficult for humans in early days of artificial intelligence. Artificial intelligence has coursed through the following phases before turning the milestone of self-taught machines [46]:

Knowledge based AI: This approach of AI required the programmers to feed the machine with all the details about the problem. Surprisingly the use of knowledge base approach made a number of monotonous tasks easier for machines to solve. Through *knowledge base* approach to artificial intelligence (AI), computers have defeated even the best chess player, Garry Kasparov [47].

Machine Learning: Solving intuitive and subjective problems, such as recognizing voices and contents of an image, proved to be a taxing task for AI. Solution of such intuitive tasks required immense amount of knowledge about the surrounding world and a large database of decision statements. These challenges suggested that instead of hard-coded knowledge, AI systems required to develop self-learning ability from raw data. This concept surfaced as the field of machine learning. Performance of machine learning algorithms was primarily dependent on representation of data provided to them. Maiden machine learning algorithms required manual representation of data in the form of features. The algorithms deduced results on the basis of correlation between features and output. Logistic regression and Naïve Bayes are examples of machine learning algorithms.

Representation Learning: Hand crafting of features for tedious tasks is laborious and time consuming. It may take decades for a community of researchers to devise maximally correlated features for such complex tasks. This problem was tackled by the development of representation learning which is learning of mapping from initial representation of data to an intermediate representation and then back to the original representation. A classic example of representation learning is auto-encoder.

Deep Learning: Many *factors of variation* are associated with learned features in case of representational learning. An example of factors of variation is the different viewing angles with which an image of a car is captured. Concepts of deep learning or experience based learning come handy in solving this crucial problem of representation learning. Hierarchical nature of deep learning techniques allows building of complex concepts out of simpler ones. Quintessential example of deep learning technique is feed forward network termed as multi-layer perceptron (MLP). These

Table 2
Performance metrics for retinal image analysis.

Performance metric	Description
Sensitivity (SN)	Ratio of classified true positives to the actual true positives in the ground truth. Also known as true positive rate (TPR)
Specificity (SP)	Ratio of classified true negatives to the actual true negatives in the ground truth. (1-SP) is also known as false positive rate (FPR)
Receiver Operating Characteristic curve (ROC)	Mapping of TPR to FPR at different threshold levels or mapping SN to SP in a 2 dimensional plane
Area Under the Curve (AUC)	Area covered by ROC curve when optimality is achieved

techniques are well established in audio recognition, natural language processing, and automatic speech recognition [48].

Benefits of deep learning are achieved through the use of DNN. It is a form of artificial neural network (ANN) in which arrangement of neurons is inspired by neuron disposition of animal visual cortex. DNN provide the following major commendatory advantages:

1. Hierarchical feature extraction i.e. no need of handcrafted features.
2. Limited pre-processing of input images

DNN have three kinds of layers: input layer, hidden layers, and output layer. Each layer has non-linear units known as nodes which help in modeling of complex features. DNN can learn features by following either the supervised learning method or the unsupervised method. A brief introduction of these methods is listed under the following rubrics.

3.1. Supervised learning

In supervised method DNN is provided with training data along with output labels and network tries to learn labeling using a specified learning method under the supervision of available ground truths. Classification problems are solved using supervised learning approach.

As cortical neurons in animals consider a restricted region of space to generate response, similarly neurons of CNNs respond to a restricted region of input image known as *receptive field*. This receptive field can be viewed as an image processing filter or kernel. Receptive fields are overlapping, to give an effect of sliding over input image. Response is generated by convolution of receptive field of neuron with weight matrix (generated by individual weights of neurons in same layer). Each node of input layer gets an input image patch, and output is generated for central pixel of patch as shown in Fig. 4. Output label maps for all pixels of input image patch can also be generated simultaneously using *structured prediction* method.

Usually CNNs have convolutional layers, pooling layers, and a terminating classification layer. *Pooling layers* are used to reduce dimension of feature vector which further increases computational efficiency of the network as shown in Fig. 4c. Softmax, Linear Support Vector Machine (LSVM), multi-class SVM, random forest etc. can serve the purpose of classification layer. CNNs have many variations depending on number of layers, pooling, and classifier. These include LeNet-5, VGG-16, and GoogleNet etc.

3.2. Unsupervised learning

This approach is used for pattern recognition. Unsupervised DNNs also have input layer, hidden layers, and output layer. These layers can be partially or fully connected, we can also have a terminating fully connected classification layer. Unsupervised DNN take input image and compress it, their principle is to reconstruct input image from compressed version of input image. This reconstruction is probabilistic. A number of network variants exist which include: auto-encoders, stacked auto-encoders, stacked de-noised auto-encoders, restricted Boltzmann machines etc. Usually noise is added in input images and stacked de-noising auto-encoder is then used to reconstruct original image from compressed noisy image.

3.3. Challenges to deep learning

In recent years deep learning techniques have emerged as revolutionary methods which have surpassed most of the state-of-the-art-methods. The ability of deep networks to exploit simple as well as complex compositional features of data representations is referred to as the reason behind their success. Notwithstanding, there are some issues with deep learning techniques which are yet to be solved.

3.3.1. Lack of real cognizance behind deep learning techniques

Despite achieving remarkable performance, the real cognizance behind the achievements of deep learning has remained unknown. A small number of efforts have been put forth by researchers to understand how deep networks achieve such exceptionally good results. However, there is a utmost need to develop a comprehensive theoretical background about tuning and performance assessment strategies of deep networks [49]. The following questions are still unanswered.

i. How to choose features to be extracted?
ii. How to tune parameters of network models?

3.3.2. Difficult training

Training of DNN has always remained a difficult task as there are numerous chances that they network may get stuck in local optima. Moreover, training of deep networks is very slow and requires massive computational resources for both medium and large sized data-sets to reach performance of state-of-the-art performance especially in case of offline learning. Once trained the network becomes non-adaptive for new data [49].

4. Learning methods applied for retinal image analysis

In this survey, we have reviewed 34 articles which have demonstrated the use of deep learning based techniques for classification/segmentation of retinal anatomical structures and detection of retinal diseases. A gist of every article is presented which encompasses the main focus of the reviewed manuscript. The proposed deep learning based algorithms are classified into two main classes i.e. (i) supervised learning algorithms (ii) unsupervised learning algorithms. However, these two main classes are further categorized into the following types: (i) Retinal vasculature classification/segmentation (ii) Exudates Classification/Segmentation (iii) Microaneurysm Classification (iv) Simultaneous segmentation of retinal anatomical structures (v) Simultaneous segmentation of retinal pathologies (vi) DR Identification/Classification (vii) Retinopathy of Prematurity Identification (viii)

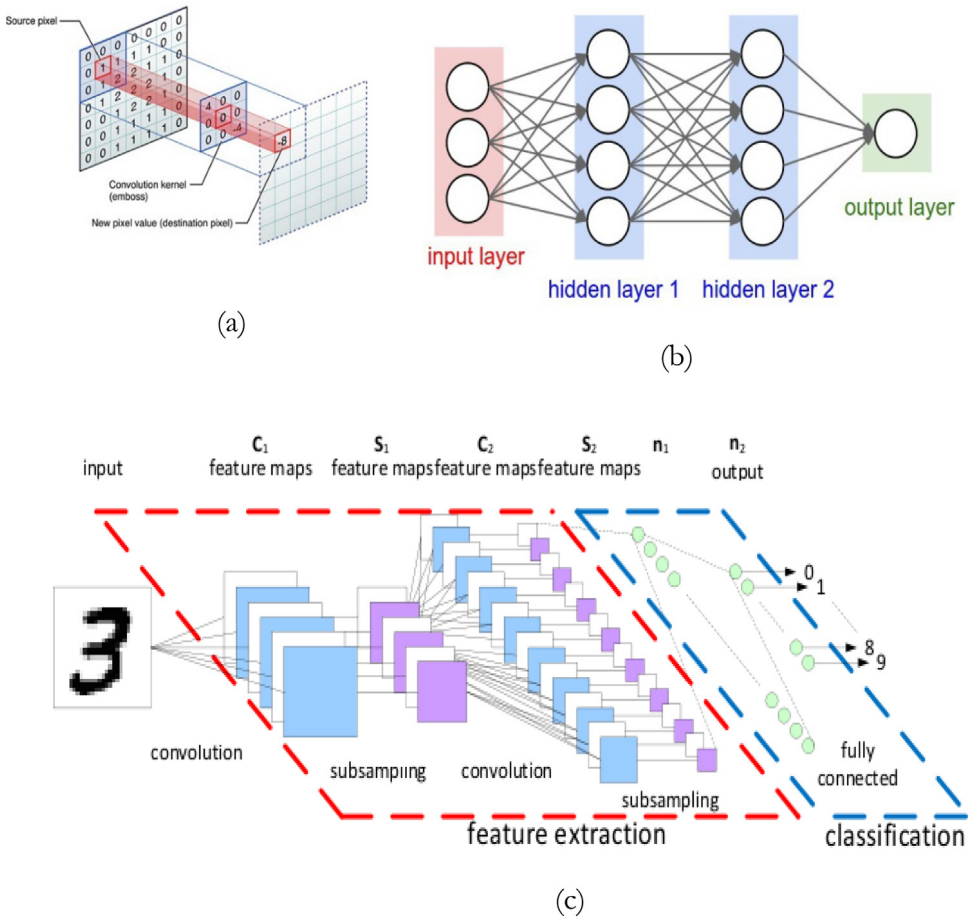

Fig. 4. Deep Neural Networks (a) Receptive field of CNN (b) Supervised CNN (c) Structure of CNN (http://swinghu.github.io/deep_learning/2015/10/09/dl-tutorials.html).

AMD Identification/Classification (ix) Multiple Retinal Disease Classification. Table 3 shows a summary of the reviewed articles including the author names, year of publication, data sources used for validating the proposed algorithms, proposed methodology, and the main focus. The methodology followed by each manuscript is discussed in the following subsections. Moreover, a quantitative performance comparison table is provided at the end of each subsection which provides the detail of the database sources used for performance evaluation and statistical results in terms of sensitivity, specificity, accuracy, and area under ROC curve.

4.1. Segmentation of retinal vasculature

4.1.1. Supervised methods

Supervised Retinal vessel segmentation problem can be broken down into two stages: (i) feature extraction, (ii) classification. Wang et al. [50] have exploited the same approach with CNN as a hierarchical feature extractor. They used ensemble random forest, which has good generalization ability, as a classifier. This classifier gives a binary output for each pixel as vessel pixel or background pixel. The green channel of RGB images contains the best retinal vessel and background contrast therefore green channel of images is used in the proposed methodology. Histogram equalization and Gaussian smoothing filter are utilized to reduce the noise and normalize uneven illumination in images. Training of network is compute intensive therefore super-pixel based sample selection is done using Simple Linear iterative clustering (LISC). The network has five layers (classic LeNet5) with one fully connected output layer. Features learned from intermediate subsampling layers and last fully connected layer are fed into three random forest classifiers. After training of CNN, each random forest is trained with learned features extracted from the network. An ensemble classifier with winner-takes-all strategy has been employed after complete training of random forest classifiers. DRIVE and STARE datasets are used to test efficacy of proposed method. Table 4 shows average case performance metrics of algorithm for both datasets. Robustness of algorithm is inspected using cross training. Accuracy in case of DRIVE (trained on STARE) is 98.03% and for STARE (trained on DRIVE) accuracy is 97.10%.

Classification of each pixel as vessel or non-vessel poses two problems: (i) system is not robust to pathology presence and (ii) pixel–pixel training of network is exhaustive. These problems can be efficiently handled by structured prediction i.e. output label map for all pixels in input image patch instead of a single label for central pixel. This approach is presented in detail by Fang et al. [51]. Their DNN has five layers with three hidden layers, network is made wide to make feature extraction effective. To allow learning of complex relationship between cross-modalities, input image patch and output label map, network is made deep. The label map is used to construct probability map which is of the same size as that of original retinal image. Probability map is enhanced by histogram equalization. Enhanced probability map is smoothed with Gaussian kernels of varying standard deviation to get different scale space images. This approach is more objective and results are not affected by image noise and other unwanted image artifacts. Results are tested on DRIVE dataset and compared with state-of-the-art SIFT and COSFIRE methods. The proposed method has superseded the traditional methods in identification of bifurcation points, extreme curvature and cross-over points.

Table 3
Deep learning based retinal image analysis methods.

Algorithm	Year	Dataset	Method	Focus	
Wang et al. [50]	2015	DRIVE, STARE	Supervised	Retinal vasculature Classification/ Segmentation	Healthy and Abnormal Retinal Anatomy Classification/Segmentation
Fang et al. [51]	2015	DRIVE			
Melinščak et al. [52]	2015	DRIVE			
Fu et al. [53]	2016	DRIVE, STARE, CHASE_DB1			
Liskowski and Krawiec [54]	2016	DRIVE, STARE			
Li et al. [55]	2016	DRIVE, STARE, CHASE_DB1			
Yao et al. [56]	2016	DRIVE			
Dasgupta and Singh [57]	2016	DRIVE			
Welikala et al. [58]	2017	UK Biobank			
Xu et al. [59]	2018	DRIVE			
Maji et al. [60]	2015	DRIVE	Hybrid		
Li et al. [55]	2016	DRIVE, STARE, CHASE_DB1			
Lahiri et al. [61]	2016	DRIVE	Unsupervised		
Prentašić and Lončarić [62]	2016	DRiDB	Supervised	Exudates Classification/ Segmentation	
Abbasi-Sureshjani et al. [63]	2017	DR2, DIARETDB1, E-Ophtha-EX			
Gulshan et al. [64]	2016	DIARETDB	Unsupervised	Microaneurysm Classification	
Maninis et al. [65]	2016	DRIVE, STARE, DRIONS-DB, RIM-ONE	Supervised	Simultaneous segmentation of retinal anatomical structures	
Tan et al. [66]	2017	DRIVE			
Zilly et al. [67]	2017	DRISHTI-GS, Messidor, RIM-ONE			
Tan et al. [68]	2017	CLEOPATRA	Supervised	Simultaneous segmentation of retinal pathologies	
Lam et al. [69]	2018	E-Ophtha			
Badar et al. [70]	2018	Messidor			
Pratt et al. [71]	2016	Kaggle	Supervised	DR Identification/ Classification	Retinal Disease Classification
Abràmoff et al. [72])	2016	MESSIDOR-2			
Gulshan et al. [64]	2016	EyePACS-1, MESSIDOR-2			
Colas et al. [73]	2016	Kaggle DR dataset			
Gargeya and Leng [74]	2017	MESSIDOR, E-OPHTHA			
Worrall et al. [75]	2016	Private dataset	Supervised	Retinopathy of Prematurity Identification	
Burlina et al. [76]	2016	NIH AREDS	Supervised	AMD Identification/Classification	
Burlina et al. [77]	2017	NIH AREDS			
Lee et al. [78]	2017	Private Dataset			
Choi et al. [79]	2017	STARE	Supervised	Multiple Retinal Disease Classification	
Arunkumar and Karthigaikumar [3]	2017	ARIA	Unsupervised		

Melinščak et al. [52] also presented a DNN for classification of retinal vasculature. Their Network has four blocks of alternating convolutional and max pooling layers with two fully connected layers at the end. Convolutional layers have ReLU activation function and last fully connected layer has Softmax activation function. The DRIVE dataset is used for training of network. Vessels are extracted from green channel of raw input images i.e. no pre-processing. Moreover, Backpropagation algorithm is used for training of network. The statistical measures obtained after testing of network are shown in Table 4.

Fu et al. [53] formulated the problem of vessel extraction as a boundary detection problem. They constructed probability maps by a fully connected four layered CNN named as DeepVessel. Convolutional layers of the proposed network have ReLU activation function. The network is a modification of holistically-nested edge detection (HED) network [80]. Probability maps from all side-output layers are fused together and a single probability map is generated. The fully connected Conditional Random Fields (CRF) are used for precise localization of vasculature boundaries. CRF is formulated as a Recurrent Neural Network (RNN). Maximum posterior marginal inference is obtained through mean field approximation of CRF distribution. The network is fine-tuned with ARIA dataset. Results obtained after evaluation of algorithm using DRIVE and STARE datasets are presented in Table 4.

Table 4
Performance measures for classification/Segmentation of Retinal vasculature using Supervised/Hybrid/Unsupervised learning Methods.

	Dataset	SN	SP	Acc	AUC	Method
Wang et al. [50]	DRIVE	81.73%	97.33%	97.67%	94.75%	Supervised
	STARE	81.04%	97.91%	98.13%	97.51%	
Melinščak et al. [52]	DRIVE	–	–	94.66%	97.49%	
Fu et al. [53]	DRIVE	76.03%	–	95.23%	–	
	STARE	71.42%	–	95.85%	–	
	CHASE_DB1	71.30%	–	94.89%	–	
Li et al. [55]	DRIVE	75.69%	98.16%	95.27%	97.38%	
	STARE	77.26%	98.44%	96.28%	98.79%	
	CHASE_DB1	75.07%	97.93%	95.81%	97.61%	
Yao et al. [56]	DRIVE	77.31%	96.03%	93.60%	–	
Dasgupta and Singh [57]	DRIVE	76.91%	98.01%	95.33%	97.44%	
Liskowski and Krawiec [54]	DRIVE	81.49%	97.49%	95.30%	97.88%	
	STARE	90.75%	97.71%	97%	99.28%	
Welikala et al. [58]	UK Biobank	–	–	86.97%	–	
Xu et al. [59]	DRIVE	87%	98%	–	–	
Li et al. [55]	DRIVE	75.69%	98.16%	95.27%	97.38%	Hybrid
	STARE	77.26%	98.44%	96.28%	98.79%	
	CHASE_DB1	75.07%	97.93%	95.81%	97.61%	
Maji et al. [60]	DRIVE	–	–	92.37%	–	
Lahiri et al. [61]	DRIVE	–	–	95.3%	–	Unsupervised

Another supervised learning method for segmentation of retinal vasculature has been proposed by Yao et al. [56]. Their network contains three convolutional layers, three intermediate pooling layers, one fully connected layer and a terminating softmax classification layer. The preliminary weight initialization is done with Gaussian distribution of specified mean and variance whereas further weight learning is done via backpropagation. The output of softmax layer is confidence level, being blood vessel pixel, with values in the range (0, 1). Classification is perfected by two stage binarization based on three dimensional characteristics of input image; confidence level image from CNN, green channel of RGB retinal input image, and their difference. The initial binarization is done by global thresholding of image which classifies each pixel as belonging to vessel class or non-vessel class. The local binarization is employed with respect to pixel-class centroid distance. This two stage binarization results in formation of unwanted artifacts which can be removed through morphological post processing i.e. erosion. Structuring elements of varying sizes are used for post processing procedure. Efficacy of algorithm is validated using DRIVE dataset. Results, as shown in Table 4, are comparable to human observer performance measures.

Dasgupta and Singh [57] provided an improved version of supervised structured prediction based multi label method for retinal vessel segmentation. Their CNN has 6 layers including a max pooling layer, an unsampling layer, and a final fully connected softmax layer. Each convolutional layer uses ReLU as an activation function. Input layer of network is fed with preprocessed green channel extracted image patches. Pre-processing steps include: image normalization, Contrast Limited Adaptive Histogram Equalization (CLAHE), and gamma adjustment. The DRIVE dataset is used for training and testing purposes. This dataset has small number of images therefore; neuron dropout method is used for increasing robustness of network. The results obtained after testing are depicted in Table 4.

Liskowski and Krawiec [54] have compared single pixel classification and structured prediction (SP) based segmentation of vessels. This extensive study is based on different network architectures and pre-processing techniques. The uneven illumination in input image patches is normalized through global contrast normalization (GCN). Zero phase component analysis (ZCA) is employed for the purpose of single pixel based classification. Neighboring pixels, in normalized image patches, are uncorrelated by multiplication of data matrix with whitening matrix. To increase the number of input samples, normalized and uncorrelated input patches are augmented. Six different types of CNN architectures are developed: PLAIN, GCN, ZCA, AUGMENT, NO-POOL, and BALANCED. As the name suggests NO-POOL network has no intermediate pooling layers, it has four preliminary convolutional layers and four fully connected layers. The PLAIN architecture has two initial convolutional layers followed by a max-pooling layer which is further followed by 2 convolutional layers, one max-pooling layer and three fully connected layers. GCN, ZCA, AUGMENT architectures are exact replica of PLAIN, they differ in training set-up. For BALANCED network, PLAIN network is trained with equal share of decision classes. Output units have sigmoidal activation whereas hidden layers have ReLU activation units. Single pixel based segmentation method is verified on DRIVE AND STARE datasets and results are presented in Table 4.

For structured prediction, network architecture is same as that of NO-POOL architecture except that the last layer is replaced by s^2 neurons and is fully connected with the second last layer. This set-up is done for construction of label map. BALANCED and NO-POOL configurations are considered for structural prediction. DRIVE and STARE datasets are used for validation of algorithm; results are shown in Table 4.

Structured prediction is more sensitive to false negatives i.e. it is less sensitive to segmentation of fine vessels. On the contrary non structured prediction is reliable for reconstruction of retinal vasculature because it gives less false negative errors.

Classification of retinal vessels into arterioles and venules also plays a pivotal role in diagnosis of many systemic, microvascular, and ophthalmic diseases. Welikala et al. [58] proposed a robust deep learning based method for classification of arterioles and venules across the entire retinal image considering the vessels located at OD. Proposed network contained 6 layers including 3 convolutional layers and 3 fully connected layers. This method was evaluated on the UK Biobank (large population-based cohort study of middle aged and older adults) dataset. In case of arterioles classification, the network achieved 86.07% of sensitivity, 87.67% of specificity, and 86.97% of accuracy whereas, for venules classification it achieved 87.67% of sensitivity, 86.07% of

specificity, and 86.97% of accuracy. Results are also presented in Table 4.

Xu et al. [59] proposed a fully convolutional neural network inspired from U-net architecture for simultaneous segmentation of arterioles and venules from retinal image. Proposed network takes colored image as input and outputs arterioles and venules with colored labels. The network was trained and tested on publicly available dataset DRIVE and outperformed the other state-of-the-art methods. Sensitivity and specificity of 87% and 98% respectively are achieved for overall vessel segmentation as illustrated in Table 4. The misclassification rates of 9.8% and 23.7% are recorded for venules and arterioles respectively.

4.1.2. Hybrid methods

The literature provides combination of supervised and unsupervised methods for segmentation of retinal blood vessels. Such an approach has been proposed by Li et al. [55]. Their DNN has five layers with three hidden layers; initially weights of first layer are obtained by pre-training of a de-noising auto-encoder (DAE) while the rest of the weights are randomly initialized. This unsupervised technique is used for weight initialization because naïve learning of weights through backpropagation has high probability of erroneous convergence into local minima. After weight initialization, overall learning and fine tuning of weights is done using backpropagation algorithm. Network is trained with a batch size of 100 and 30 epochs. Instead of using hessian matrix, vessel segmentation is done via thresholding of probability map. The proposed methodology is tested through ROC analysis using three datasets: DRIVE, STARE, and CHASE_DB1 and results are presented in Table 4. However, methodology is also tested by cross training of network i.e. testing of one dataset on network trained by other two datasets. With this experiment, accuracy measure decreased from 95.81%, 96.28%, and 95.27% to 94.17%, 95.35%, and 94.85% for the CHASE_DB1, STARE and DRIVE datasets when they are trained on DRIVE, CHASE_DB1 and STARE datasets, respectively. Cross training gives an estimate for feasibility criteria of algorithm from clinical point of view.

Another hybrid methodology is formulated by Maji et al. [60] using an unsupervised training followed by supervised classifier training for retinal vessel segmentation. They have used two DAEs followed by an RF classifier for extraction of vessels. The unsupervised pre-training of stacked auto-encoder is used for learning weights of network. Once pre-training is done, an ensemble RF classifier is trained in a supervised manner in the presence of ground truth. The presented algorithm is tested on DRIVE dataset. The maximum accuracy obtained is 92.37% as depicted in Table 4. The results obtained are not good compared to traditional methods but they give a state-of-the-art for hybrid DNNs.

4.1.3. Unsupervised methods

Retinal vessel segmentation can also be done using unsupervised deep learning methods, although this field is not that much explored but it has the potential to surpass statistical measures obtained from current state-of-the-art methods.

Lahiri et al. [61] has presented a two level SDAE network for retinal vessel segmentation. CLAHE is employed to get rid of uneven illumination. A simple DAE has three layers with one hidden layer. Random noise is deliberately added in the input to achieve unsupervised learning. L-BFG (Limited Memory Broyden–Fletcher–Goldfarb–Shanno) is used to update the weight matrix. SDAE is obtained by taking hidden layer output of first DAE as input to second DAE and training it. The first level of ensemble is formed by making a collection of n DAEs termed as E1.net. Multiple DAE kernels allow the vessel feature learning in multiple directions. An SDAE (2 hidden layers) with Softmax classified output makes the second level of ensemble. Further diversification is added by parallel training of two E1.nets with different architecture. Convex weighted average is used to get the combined decision of both E1.nets. The algorithm is tested using publicly available DRIVE dataset. The maximum average accuracy is recorded at 95.3% and Kappa agreement coefficient at 70.9% as presented in Table 4. This method outperformed the human observer accuracy which was recorded at 94.7%.

4.2. Segmentation of exudates

4.2.1. Supervised methods

Exudates, lipids and lipoproteins are pre-eminent signs of DR. The exudates are of varying sizes, they can vary from very small size to the size as large as that of an OD. DNNs provide worthwhile provisions for detection of exudates in retinal fundus images. Prentašić and Lončarić [62] have presented a DNN architecture in their study for automatic detection of exudates. Their network has ten alternating convolutional and max pooling layers. A Softmax activation function is used after the last layer to provide probability based classification of individual pixels i.e. exudate or non-exudate class. Network is fed with green plane of RGB retinal image. They combined probability maps from DNN with other landmark detection probability maps to exploit the domain knowledge i.e. exudates do not appear inside retinal blood vessels and OD. The OD detection probability map is obtained from an ensemble of strategies which include: entropy based approach, Laplacian of Gaussian approach, brightness approach [81], and Hough transformation method. Blood vessel probability map is generated by using Frangi [82] vesselness filter. After blood vessel and OD detection a parabola is fitted at the center of OD which encapsulates the regions where there is less potential of exudate presence. At the time of training, input image is de-noised using total variation (TV) regularization de-noising. DRiDB data is used for training and testing of deep network. Table 5 shows the statistical results obtained after testing.

An arrangement of CNN, which is a modification of bag-of-visual-words (BoVW) method, for detection of DR is communicated by Costa and Campilho [83]. The significance of the method lies in the advantage that the method is capable of performing feature extraction, feature encoding and classification jointly unlike the traditional BoVW. They used DR2 and Messidor datasets to check the usefulness of their method.

Deep learning in small data regime i.e. training of time consuming and high sample complexity algorithms using limited resources is the need of the hour in medical image analysis. This kind of methodology has been proposed by Otálora et al. [84] in their work for exudate classification. They provided a label efficient CNN along with an active learning algorithm, expected gradient length (EGL). EGL provided a degree of freedom to the learner by allowing selection of instances to be labeled and added to the training set from a set of unlabeled instances. EGL performed better than the usual stochastic gradient descent because it helped in earlier convergence of CNN training by feeding the network with the most informative patches from retinal images. The CNN model was based on LeNet network and it was trained using transfer learning approach. Moreover, the efficacy of the algorithm was tested using a publicly available data-set E-Ophtha. However, this algorithm poses a computational drawback when the number of unlabeled instances are large.

The number of false positives in the segmentation of exudates from retinal images can be reduced by using importance sampling approach. This approach has been followed by [63] in their work for boosted exudates segmentation. Importance sampling is concerned with prioritizing the sampling towards non-exudate samples that could mislead the network during training. This avoids the need of any post-processing steps. The

Table 5
Performance measures for Classification/Segmentation of Exudates using Supervised learning Methods.

	Dataset	SN	SP	Acc	AUC
Prentašić and Lončarić [62]	DRiDB	78%	–	–	–
Abbasi-Sureshjani et al. [63]	DR2	–	–	–	97.2%
	DIARETDB1	–	–	–	96.5%
	E-Ophta-EX	–	–	–	99.4%

Table 6
Performance measures for Classification/Segmentation of Microaneurysms using Unsupervised learning Methods.

	Dataset	SN	SP	Acc	AUC
Gulshan et al. [64]	DIARETDB1	–	91.60%	91.38%	96.20%

proposed methodology was based on a CNN with 9 ResNet blocks. The retinal images were enhanced using Gaussian kernel before feeding them to the network whereas the network weights were optimized using stochastic gradient descent [85]. Table 5 contains the statistical results obtained by evaluating the algorithm. The testing of the network resulted in AUC of 97.2%, 96.5%, and 99.4% when it was evaluated against three publicly available data-sets i.e. DIARETDB1, DR2, and E-Ophtha-EX respectively.

4.3. Segmentation of microaneurysms

4.3.1. Unsupervised methods

Microaneurysms rupture retinal blood vessels and make blood to leak from them. These miniature lesions appear as early signs of DR, therefore, they play a pivotal role in timely detection of DR. Automatic extraction of these lesions from 2-D fundus images has been demonstrated by Gulshan et al. [64]. Extraction of microaneurysms features is done straightaway from raw image patches i.e. no pre-processing is applied. Image patches are segregated into two classes i.e. lesion present and non-lesion present. Sampling of image patches is done from green channel of input image. Computer-aided feature extraction is done with the help of SSAE and Softmax classifier is used to label features. Two hidden layers constitute SSAE. First layer is used to extract features from raw image patches and second layer learns intricate features from output of first layer. Softmax binary classifier is connected with second layer of SSAE. Algorithm is scrutinized with the help of DIARETDB1 dataset. Classification results from Softmax classifier are tuned by varying patch-sizes. Fine tuning has provided steady state and more efficient results as compared to previous ones. Results, as depicted in Table 6.

4.4. Simultaneous segmentation of retinal landmarks and pathologies

4.4.1. Supervised methods

Simultaneous segmentation of retinal landmarks as well as pathologies is also possible through the use of DNNs. Maninis et al. [65] presented the problem of landmark detection as image–image regression problem. They formulated a variation of VGG-16 DNN for segmentation of OD and retinal blood vessels. The network is inspired from VGG except that last fully connected layer is removed. It has 5 stages with multiple convolutional layers with ReLU activation and intermediate max pooling layers. Network weights are learned by backpropagation algorithm and stochastic gradient descent. To increase generalization ability of network; dataset is augmented with rotated and scaled versions of input images. Efficiency of algorithm towards blood vessel detection is scrutinized using DRIVE and STARE datasets whereas OD segmentation is tested using DRIONS-DB and RIM-ONE dataset. For DRIVE dataset the method achieved 82.2% F1-measure and for stare F1-measure is recorded at 83.1%. OD segmentation using DRIONS-DB dataset achieved 97.1% F1-measure while that of RIM-ONE is found to be 95.9%.

Tan et al. [66] have recommended and tested a CNN based deep network for concurrent segmentation of OD, fovea and retinal blood vessels. Three convolution layers with intermediate max pooling layers constitute the model. Each layer has leaky ReLU activation units. Last fully connected layer has Softmax activation unit. Layer one weights are initialized using Xavier initialization algorithm [86]. Network is trained using backpropagation and stochastic gradient descent. Before any classification input images are normalized using L channel of LUC color space, then images are converted back to RGB color space and green channel is extracted for further processing. Training and testing of network is conducted on DRIVE dataset and Outcomes are articulated in Table 7.

The segmentation of OD and cup is very important for finding the Cup to Disc Ratio (CDR) which is an essential indicator of glaucoma progression. Zilly et al. [67] have presented a CNN architecture based on ensemble learning. Instead of backpropagation, they have used a greedy approach in which boosting is used to learn weights of each stage. Moreover, for training the network, they have introduced the use of entropy sampling as a substitute of uniform sampling. Entropy sampling helps the network in focusing on the most informative points in the image. Also, because of entropy sampling their network has the capability to be trained using a smaller dataset. They have investigated the efficacy of their algorithm using DRISHTI-GS [87], Messidor and RIM-ONE datasets. For RIM-ONE dataset, the proposed methodology recorded sensitivity, specificity and accuracy of 92.3%, 95.6%, and 94.1% for glaucoma classification using the CDR values.

Simultaneous segmentation of retinal pathologies can also be done using multi class CNNs. This approach has been adopted by Tan et al. [68] in their work. They formulated a 10 layered neural network for automated segmentation of exudates, microaneurysms, and hemorrhages from retinal fundus images. The leaky rectified linear unit was employed as an activation function for convolutional and fully connected layers whereas softmax function was used for final fully connected layer. Moreover, the network was trained using back propagation and stochastic gradient descent and regularization was espoused to avoid overfitting. The retinal images were normalized for uneven illumination correction and local contrast adjustment before feeding them to network. This CNN based technique is data-dependent because the deep learning techniques crave for a large number of training samples. The proposed algorithm is evaluated with a new dataset named as CLEOPATRA and the results are illustrated in Table 7.

Lam et al. [69] presented a method of localizing and delineating multiple types of pathologies in retinal images. They trained standard CNNs like VGG-16, AlexNet, ResNet, GoogLeNet, and Inception-v3 on selected image patches from Kaggle dataset. The final CNN is selected in the basis of the obtained accuracy. The method is used to predict the presence of exudates, cotton wool spots, hemorrhages, microaneurysms, and neovascularization in the test image patches. The methodology is validated using the E-Ophtha dataset. In case of pixel wise classification, the proposed algorithm attained AUC of 94% and 95% whereas with lesion-wise classification AUC of 86% and 64% is achieved for microaneurysms and hard exudates, respectively. The obtained performance measures are also presented in Table 7.

A more efficient method for simultaneous segmentation of retinal pathologies has been presented by Badar et al. [70]. They proposed an encoder decoder based fully deep CNN inspired by

semantic segmentation network Segnet [88]. Proposed network was used to semantically segment retinal pathologies i.e. exudates, hemorrhages, and cotton-wool spots and assign each pixel of the retinal image a class label such as background, exudates, hemorrhages, and soft exudates. The network was trained and tested on a subset of publicly available dataset Messidor and achieved state-of-the-art accuracies. The segmentation results obtained by the proposed methodologies are recorded in Table 7.

4.5. Retinal disease classification

Distinctive characterization of retinal diseases requires experienced clinicians but the advancement in the fields of image processing and machine learning helped in completely automating this process. As the traditional methods for automatic classification of retinal diseases reached excellence, advent of deep learning has provided afresh way for efficient and accurate diagnosis of retinal diseases. The literature has provided supervised and unsupervised methods for automatic classification of retinal diseases using deep learning techniques. The details of the so far proposed works are discussed in the proceeding sections.

4.5.1. Supervised methods

An automated screening algorithm, using supervised deep learning technique, for classification of DR into severe, proliferative, and non-proliferative is recommended by [73]. They developed a DNN for this purpose. The algorithm is tested using Kaggle DR Detection challenge dataset. This dataset has 10,000 images captured from 5000 patients. The algorithm achieved an AUC of 94.6%, sensitivity of 96.2%, and 66.6% specificity as presented in Table 8.

Pratt et al. [71] have provided a DNN for identification and classification of DR into four categories: mild DR, moderate DR, severe DR, and proliferative DR. Their deep network extracts deep features from retinal image which are then used for classification of DR. The proposed network has ten convolutional layers with intermediate max pooling layers followed by two fully connected and a Softmax classification layer. Each layer has leaky ReLU activation unit and L2 normalization for weights and biases. Color normalization, using OpenCV package, is done to even out unnecessary variations in input images. Gaussian initialized weights are batch normalized after each layer. To avoid over fitting, weighted class weights and node dropout strategy is used. Network is trained through stochastic gradient descent and Nestrov momentum weight learning methods. After pre-training, network is further trained with real time augmented image patches. This is done to improve localization ability of system. Legitimacy of algorithm is tested on Kaggle dataset. Proposed method provided 95% sensitivity and 75% accuracy as presented in Table 8.

Abràmoff et al. [72] provided an improved version of their previous work for classification of DR and ME, older version of algorithm was developed without incorporating deep learning. New algorithm provides automatic identification and Classification of DR into moderate, severe non proliferative DR (NPDR), proliferative DR (PDR), and ME with improved statistical measures. They used IDX-DR version X2.1 automated system. The device was trained using EyeCheck project dataset. Evaluation of system is done using Messidor-2 dataset. The statistical findings are presented in Table 8.

A method for identification of DR and diabetic ME from retinal fundus images has been provided by Gulshan et al. [64]. They used Inception v3 DNN architecture [89]. EyePACS-1 and MESSIDOR-2 datasets are used for training and testing of network. ImageNet dataset is used for initialization of network weights. The weights are learned via distributed stochastic gradient and training of network is made efficient by using batch normalization. Algorithm is inspected using two operating points. Focus of first operating point is high specificity and that of second is high sensitivity. Results obtained are shown in Table 8.

Clinician could be aided in grading of DR through a visualization heatmap. Gargeya and Leng [74] have provided an automated CNN based model for grading of DR and they also generated heatmap for easy abnormality detection by clinicians. Network has convolutional blocks with 4, 6, 8, and 10 layers. Each layer incorporates batch normalization and ReLU activation units. Last layer is Softmax classification layer preceded by an average pooling layer and a visualization layer. Heatmap is generated using visualization layer which has functionality similar to that of a convolutional layer. Training of model is done on EyePACS dataset. Input images are normalized, downsized and augmented to reduce the unnecessary varying brightness and contrast. Some meta-data, related to original image, is appended with feature vector to normalize the effect of environmental variables. Algorithm provided 97% AUC, with 94% and 98% sensitivity and specificity respectively for EyePACS dataset. Generalization ability of algorithm is tested using MESSIDOR-2 and E-OPTHA datasets. Results are presented in Table 8.

Retinopathy of Prematurity (ROP) is one of the largest preventable cause of blindness in children. Therefore, early diagnosis of ROP plays an imperative role in the prevention of childhood visual loss. Worrall et al. [75] have recommended a deep CNN for detection of ROP. They are the first who have proposed a deep learning based end to end system for early diagnosis of ROP. They fine-tuned the pre-trained GoggleNet and used it as a detector of ROP. The accuracy of the CNN is improved with the help of a Bayesian framework. They have also employed pre-processing and augmentation of retinal images. The network is trained and tested using a private database. The statistical performance evaluation resulted in 93.6%, 95.4%, and 94.7% of sensitivity, specificity, and accuracy respectively as shown in Table 8.

Identification of AMD is a crucial task. Silent nature of the disease, during intermediate stage, results in asymptotic severity leading to complete vision loss. Features learnt from pre-trained neural networks can help in effective diagnosis of AMD at intermediate stage. Burlina et al. [76] have checked appropriateness of this technique for classification of AMD. Overfeat Features (OF) are extracted from pre-trained deep CNN on a generic dataset, ImageNet. Resized images are fed into the network for learning OF features. Most imperative and prognostic retinal region for AMD diagnosis is the central part of retina. This information is utilized by extracting features appended from multiple concentric square grids. LSVM is trained with extracted features. Efficiency of model is scrutinized using NIH AREDS dataset. The dataset is divided into two classes i.e. EIPC (equal number of images per class) and MIPC (maximum number of images per class). Performance is evaluated on both classes of dataset as presented in Table 8.

Burlina et al. [77] have extended their work to identify the class of AMD. Class 1 corresponds to no AMD, class 2 incorporates early stage AMD cases, class 3 encompasses intermediate stage AMD, and class 4 denotes advanced form of AMD. They have used OverFeat deep CNN for finding the severity grade of AMD. The efficacy of the algorithm is scrutinized using NIH AREDS dataset. The obtained performance measures are shown in Table 8.

3-D OCT imaging modality is the most common among imaging modalities in the field of ophthalmology. OCT images combined with electronic medical records (EMR) give a rich dataset for training of DNNs. Lee et al. [78] have followed the same footings for AMD detection. They implemented VGG-16 DNN for efficient classification of AMD using OCT images. Their network consists of 21 layers, including convolutional layers and max pooling layers, each with a ReLU activation unit. Automatically

Table 7
Performance measures for Simultaneous Segmentation of Retinal anatomical structures using Supervised learning Methods.

	Dataset	Class	SN	SP	Acc	AUC
Tan et al. [66]	DRIVE	Background	95.47%	80.63%	–	–
		OD	87.90%	99.27%	–	–
		Fovea	88.53%	99.14%	–	–
		Blood Vessels	75.73%	96.94%	–	–
Tan et al. [68]	CLEOPATRA	Hemorrhages	62.57%	98.93%	–	–
		Hard Exudates	87.58%	98.73%	–	–
		Microaneurysms	46.06%	97.99%	–	–
Badar et al. [70]	Messidor	Hemorrhages	80.93%	98.54%	97.86%	–
		Hard Exudates	90.69%	99.64%	99.24%	–
		Soft Exudates	72.87%	89.32%	88.65%	–
Lam et al. [69]	E-Ophta	Hard Exudates	–	–	–	95%
		Microaneurysms	–	–	–	94%

Table 8
Performance measures for Retinal Disease classification using Supervised/Unsupervised learning methods.

	Dataset	SN	SP	Acc	AUC	Method	Focus
Colas et al. [73]	Kaggle DR detection dataset	96.2%	66.6%	–	94.6%	Supervised	DR Identification/ Classification
Pratt et al. [71]	Kaggle DR detection dataset	95%	–	75%	–		
Abràmoff et al. [72]	MESSIDOR-2	96.8%	87%	–	98%		
Gulshan et al. [64]	EyePACS-1	90.3%	98.1%	–	–		
	MESSIDOR-2	87%	98.5%	–	–		
Gargeya and Leng [74]	MESSIDOR 2	93%	87%	–	94%		
	E-OPTHA	90%	94%	–	95%		
Worrall et al. [75]	Private dataset	93.6%	95.4%	94.7%	–	Supervised	ROP Identification
Burlina et al. [76]	NIH AREDS	90.9%–95.7%	90.1%–95.6%	91.9%–95%	–	Supervised	AMD Identification/ Classification
Lee et al. [78]	3-D OCT Images	92.64%	93.69%	93.45%	97.45%		
Burlina et al. [77]		–	–	85%	–		
Choi et al. [79]	STARE			36.7%		Supervised	Multiple Retinal diseases classification
Arunkumar and Karthigaikumar [3]	ARIA	79.32%	97.89%	87.62%	–	Unsupervised	

extracted OCT images are used for training and testing of network. Weights are initialized using Xavier algorithm [86] and optimized by stochastic gradient descent. Input images are first downsized and histogram equalized and are then fed into the network. Results are shown in Table 8.

Choi et al. [79] proposed a deep CNN for systematic detection of multiple retinal diseases using fundus photographs of STARE image set. The data set was expanded by incorporating nine more diseases such background DR, PDR, Dry AMD, Wet AMD, Retinal Vein Occlusion, Retinal Artery Occlusion, Hypertensive retinopathy, Coat's disease, and Retinitis. Initially, random forest with VGG19 transfer learning method is used to classify the diseases but due to the multiple diseases, accuracy was quite low. Later ensemble classifiers are introduced to achieve better classification accuracy of multiple diseases. The network is reported to achieve 36.7% accuracy in the classification task of nine retinal diseases.

4.5.2. Unsupervised methods

Unsupervised DNNs have proved effective for classification of retinal diseases such as: AMD, DR, Macular Bunker, Retinoblastoma, Retinal Detachment, and Retinitis Pigmentosa. This approach has been suggested by Arunkumar and Karthigaikumar [3]. They used Generalized Regression Neural Network (GRNN) for reduction of feature vector dimension. This is done to improve compute time efficiency. The model is able to extract intricate features because it includes stacked Restricted Boltzmann Machine (RBM) [90] in its layers. Input images are first preprocessed to remove noise and adjust contrast. Effectiveness of system is checked on ARIA dataset. Results are recorded in Table 8.

5. Discussion

From our survey of DNNs for retinal image analysis we can deduce that overall supervised learning approaches have performed better as compared to unsupervised learning methods because supervised learning networks learn the mapping efficiently due to the presence of ground truth data. Most of the progress in deep learning based retinal image analysis has been witnessed in the segmentation of retinal vasculature. Among all the DNN based algorithms which utilize intensity level pixel information, [55] have provided the maximum AUC of 98.79%. However, use of only intensity level information undermines the efficiency of algorithm because neighboring pixels always have a certain correlation factor. The blood vessel segmentation methodology

proposed by Liskowski and Krawiec [54] have utilized contextual information along with intensity level information of pixels for blood vessel segmentation. Because of the use of neighborhood information, their model outperformed other retinal blood vessel segmentation techniques. It achieved maximum AUC of 99.28% which is higher than best to date AUC recorded by other traditional approaches. Instead of following a tedious approach i.e. one by one retinal landmark detection, DNNs can be used for simultaneous extraction of retinal landmarks from retinal images. This approach is presented by Tan et al. [66]. DNN have not yet been much explored for retinal pathology detection. Prentašić and Lončarić [91] have provided state-of-the-art results for detection of exudates. The method proposed by Shan and Li [92] for microaneurysms detection through SSAE achieved an AUC of 96.20%. Some of the recent works have explored supervised DNNs for simultaneous segmentation of retinal pathologies. Tan et al. [68] provided a segmentation network for simultaneous segmentation of exudates, hemorrhages, and microaneurysms. Badar et al. [70] presented a better approach by providing a method for pixel level segmentation of exudates, hemorrhages, and cotton wool spots. Deep learning is still an underexplored technique in the field of retinal pathology detection. Lee et al. [78] have proved efficacy of DNN for grading of AMD in 3-D OCT images by recording an AUC of 97.45%. Supervised DNN approach have also been employed for efficient grading of DR [64,71,73,74] are examples of this effort. Among all of them, [72] have achieved the maximum AUC of 98.0% for grading of DR.

6. Conclusion

Retinal image analysis through DNNs is a nascent field. Although research has been conducted in extraction of retinal landmarks and pathologies but the epitome of this technique is yet to be witnessed. However, unsupervised learning based DNNs have not seen much progress in retinal image analysis. Deep learning techniques can be efficiently applied for segmentation of dot and blot hemorrhages, cotton wool spots, hard exudates, soft exudates, drusen etc. There is no restriction on number of layers and architecture of neural network, network architecture is chosen heuristically in accordance with problem domain. The variants of Deep Neural Networks like AlexNet, LSTM, VggNet, and GoogleNet can be used for extraction of retinal anatomical structures. Although VGG-16 is used by Lee et al. [78] for 3-D OCT retinal image analysis; however, there is no precedence of its use in case of color fundus images. All these networks are very deep and they have capability of extracting much more complex features than those extracted by traditional methods and with better performance measures. This property makes DNN capable of replacing traditional ophthalmologic screening practices.

Declaration of competing interest

The authors declare that they have no known competing financial interests or personal relationships that could have appeared to influence the work reported in this paper.

References

[1] M.M. Fraz, P. Remagnino, A. Hoppe, B. Uyyanonvara, A.R. Rudnicka, C.G. Owen, S.A. Barman, Blood vessel segmentation methodologies in retinal images–a survey, Comput. Methods Programs Biomed. 108 (1) (2012) 407–433.

[2] M.D. Abràmoff, M.K. Garvin, M. Sonka, Retinal imaging and image analysis, IEEE Rev. Biomed. Eng. 3 (2010) 169–208.

[3] R. Arunkumar, P. Karthigaikumar, Multi-retinal disease classification by reduced deep learning features, Neural Comput. Appl. 28 (2) (2017) 329–334, http://dx.doi.org/10.1007/s00521-015-2059-9.

[4] A. Sopharak, B. Uyyanonvara, S. Barman, T.H. Williamson, Automatic detection of diabetic retinopathy exudates from non-dilated retinal images using mathematical morphology methods, Comput. Med. Imaging Graph. 32 (8) (2008) 720–727.

[5] T. Walter, J.-C. Klein, P. Massin, A. Erginay, A contribution of image processing to the diagnosis of diabetic retinopathy-detection of exudates in color fundus images of the human retina, IEEE Trans. Med. Imaging 21 (10) (2002) 1236–1243.

[6] M.M. Fraz, P. Remagnino, A. Hoppe, B. Uyyanonvara, A.R. Rudnicka, C.G. Owen, S.A. Barman, An ensemble classification-based approach applied to retinal blood vessel segmentation, IEEE Trans. Biomed. Eng. 59 (9) (2012) 2538–2548.

[7] G. Quellec, M. Lamard, P.M. Josselin, G. Cazuguel, B. Cochener, C. Roux, Optimal wavelet transform for the detection of microaneurysms in retina photographs, IEEE Trans. Med. Imaging 27 (9) (2008) 1230–1241.

[8] D. Marín, A. Aquino, M.E. Gegúndez-Arias, J.M. Bravo, A new supervised method for blood vessel segmentation in retinal images by using gray-level and moment invariants-based features, IEEE Trans. Med. Imaging 30 (1) (2011) 146–158.

[9] Y. Kanagasingam, A. Bhuiyan, M.D. Abràmoff, R.T. Smith, L. Goldschmidt, T.Y. Wong, Progress on retinal image analysis for age related macular degeneration, Progress Retin. Eye Res. 38 (2014) 20–42.

[10] I. Sadek, D. Sidibé, F. Meriaudeau, Automatic discrimination of color retinal images using the bag of words approach, in: Paper presented at the SPIE Medical Imaging, 2015.

[11] D. Sidibé, I. Sadek, F. Mériaudeau, Discrimination of retinal images containing bright lesions using sparse coded features and SVM, Comput. Biol. Med. 62 (2015) 175–184.

[12] R. Veras, R. Silva, F. Araújo, F. Medeiros, SURF descriptor and pattern recognition techniques in automatic identification of pathological retinas, in: Paper Presented at the Intelligent Systems (BRACIS), 2015 Brazilian Conference on, 2015.

[13] N. Patton, T.M. Aslam, T. MacGillivray, I.J. Deary, B. Dhillon, R.H. Eikelboom, et al., Retinal image analysis: Concepts, applications and potential, Progress Retin. Eye Res. 25 (1) (2006) 99–127.

[14] D.M. Albert, W.H. Miller, Jan purkinje and the ophthalmoscope, Am. J. Ophthalmol. 76 (4) (1973) 494–499.

[15] D. Huang, E.A. Swanson, C.P. Lin, J.S. Schuman, W.G. Stinson, W. Chang, et al., Optical coherence tomography, Science 254 (5035) (1991) 1178.

[16] T.J. Bennett, C.J. Barry, Ophthalmic imaging today: An ophthalmic photographer's viewpoint–a review, Clin. Exp. Ophthalmol. 37 (1) (2009) 2–13.

[17] P. Venkatesh, R. Sharma, N. Vashist, R. Vohra, S. Garg, Detection of retinal lesions in diabetic retinopathy: Comparative evaluation of 7-field digital color photography versus red-free photography, Int. Ophthal. 35 (5) (2015) 635–640.

[18] M.E. Tyler, Stereo fundus photography: Principles and technique, J. Ophthalmic Photogr. 18 (2) (1996) 6–81.

[19] Y. Hirohara, Y. OKawa, T. Mihashi, T. Yamaguchi, N. Nakazawa, Y. Tsuruga, et al., Validity of retinal oxygen saturation analysis: Hyperspectral imaging in visible wavelength with fundus camera and liquid crystal wavelength tunable filter, Opt. Rev. 14 (3) (2007) 151.

[20] I. Alabboud, G. Muyo, A. Gorman, D. Mordant, A. McNaught, C. Petres, et al., New spectral imaging techniques for blood oximetry in the retina, in: Paper Presented at the European Conference on Biomedical Optics, 2007.

[21] R.H. Webb, G.W. Hughes, Scanning laser ophthalmoscope, IEEE Trans. Biomed. Eng. (7) (1981) 488–492.

[22] A. Roorda, F. Romero-Borja, W.J. Donnelly I.I.I., H. Queener, T.J. Hebert, M.C. Campbell, Adaptive optics scanning laser ophthalmoscopy, Opt. Exp. 10 (9) (2002) 405–412.

[23] E. Ng, U.R. Acharya, R.M. Rangayyan, J.S. Suri, Ophthalmological Imaging and Applications, CRC Press, 2014.

[24] J.S. Slakter, L.A. Yannuzzi, D.R. Guyer, J.A. Sorenson, D.A. Orlock, Indocyanine-green angiography, Curr. Opin. Ophthalmol. 6 (3) (1995) 25–32.

[25] W. Drexler, J.G. Fujimoto, Optical Coherence Tomography: Technology and Applications, Springer, 2015.

[26] F.A. Jakobiec, Ocular Anatomy, Embryology, and Teratology, Harpercollins, 1982.

[27] J. Beagley, L. Guariguata, C. Weil, A.A. Motala, Global estimates of undiagnosed diabetes in adults, Diabetes Res. Clin. Pract. 103 (2) (2014) 150–160.

[28] V. Raman, P. Then, P. Sumari, Proposed retinal abnormality detection and classification approach: Computer aided detection for diabetic retinopathy by machine learning approaches, in: Paper Presented at the Communication Software and Networks (ICCSN), 2016 8th IEEE International Conference on, 2016.

[29] R.L. Engerman, Pathogenesis of diabetic retinopathy, Diabetes 38 (10) (1989) 1203–1206.

[30] R.A. Kowluru, P.-S. Chan, Capillary Dropout in Diabetic Retinopathy Diabetic Retinopathy, Springer, 2008, pp. 265–282.

[31] M. Niemeijer, J. Staal, B. Ginneken, M. Loog, M. Abramoff, DRIVE: Digital retinal images for vessel extraction, in: Methods for Evaluating Segmentation and Indexing Techniques Dedicated To Retinal Ophthalmology, 2004.
[32] A. Hoover, V. Kouznetsova, M. Goldbaum, Locating blood vessels in retinal images by piecewise threshold probing of a matched filter response, IEEE Trans. Med. Imaging 19 (3) (2000) 203–210.
[33] ARIA Online, Retinal image archive, 2006, http://www.eyecharity.com/aria online/.
[34] T. Kauppi, V. Kalesnykiene, J.-K. Kamarainen, L. Lensu, I. Sorri, H. Uusitalo, et al., DIARETDB0: Evaluation database and methodology for diabetic retinopathy algorithms, in: Machine Vision and Pattern Recognition Research Group, Lappeenranta University of Technology, Finland, 2006, p. 73.
[35] R. Kälviäinen, H. Uusitalo, DIARETDB1 diabetic retinopathy database and evaluation protocol, in: Paper Presented at the Medical Image Understanding and Analysis, 2007.
[36] E. Decencière, X. Zhang, G. Cazuguel, B. Laÿ, B. Cochener, C. Trone, et al., Feedback on a publicly distributed image database: The Messidor database, Image Anal. Stereol. 33 (3) (2014) 231–234.
[37] P. Prentašić, S. Lončarić, Z. Vatavuk, G. Benčić, M. Subašić, T. Petković, et al., Diabetic retinopathy image database(DRiDB): A new database for diabetic retinopathy screening programs research, in: Paper Presented at the 2013 8th International Symposium on Image and Signal Processing and Analysis, ISPA, 2013.
[38] J.J. Kanski, B. Bowling, Clinical Ophthalmology: A Systematic Approach, Elsevier Health Sciences, 2011.
[39] R. Klein, M.D. Knudtson, K.E. Lee, R. Gangnon, B.E. Klein, The Wisconsin Epidemiologic Study of Diabetic Retinopathy XXIII: The twenty-five-year incidence of macular edema in persons with type 1 diabetes, Ophthalmology 116 (3) (2009) 497–503.
[40] R. Varma, N.M. Bressler, Q.V. Doan, M. Gleeson, M. Danese, J.K. Bower, et al., Prevalence of and risk factors for diabetic macular edema in the United States, JAMA Ophthalmol. 132 (11) (2014) 1334–1340.
[41] R.D. Jager, W.F. Mieler, J.W. Miller, Age-related macular degeneration, N. Engl. J. Med. 358 (24) (2008) 2606–2617.
[42] D.V. Alfaro, Age-Related Macular Degeneration: A Comprehensive Textbook, Lippincott Williams & Wilkins, 2006.
[43] G. Liew, J.J. Wang, Retinal vascular signs: A window to the heart? Rev. Esp. Cardiol. (English Edition) 64 (6) (2011) 515–521.
[44] H.A. Quigley, A.T. Broman, The number of people with glaucoma worldwide in 2010 and 2020, Br. J. Ophthalmol. 90 (3) (2006) 262–267.
[45] R. Thomas, R.S. Parikh, How to assess a patient for glaucoma, Community Eye Health 19 (59) (2006) 36.
[46] I. Goodfellow, Y. Bengio, A. Courville, Deep Learning, MIT press, 2016.
[47] F.-H. Hsu, Behind Deep Blue: Building the Computer that Defeated the World Chess Champion, Princeton University Press, 2002, http://swinghu.github.io/deep_learning/2015/10/09/dl-tutorials.html.
[48] Y. LeCun, Y. Bengio, G. Hinton, Deep learning, Nature 521 (7553) (2015) 436–444.
[49] P. Angelov, A. Sperduti, Challenges in deep learning, in: Paper Presented at the Proceedings of the 24th European symposium on artificial neural networks, ESANN, 2016.
[50] S. Wang, Y. Yin, G. Cao, B. Wei, Y. Zheng, G. Yang, Hierarchical retinal blood vessel segmentation based on feature and ensemble learning, Neurocomputing 149 (2015) 708–717.
[51] T. Fang, R. Su, L. Xie, Q. Gu, Q. Li, P. Liang, T. Wang, Retinal vessel landmark detection using deep learning and hessian matrix, in: Paper Presented at the Image and Signal Processing (CISP), 2015 8th International Congress on, 2015.
[52] M. Melinščak, P. Prentašić, S. Lončarić, Retinal vessel segmentation using deep neural networks, in: Paper Presented at the VISAPP 2015 (10th International Conference on Computer Vision Theory and Applications), 2015.
[53] H. Fu, Y. Xu, S. Lin, D.W.K. Wong, J. Liu, DeepVessel: Retinal vessel segmentation via deep learning and conditional random field, in: Paper presented at the International Conference on Medical Image Computing and Computer-Assisted Intervention, 2016.
[54] P. Liskowski, K. Krawiec, Segmenting retinal blood vessels with<? pub _newline?> deep neural networks, IEEE Trans. Med. Imaging 35 (11) (2016) 2369–2380.
[55] Q. Li, B. Feng, L. Xie, P. Liang, H. Zhang, T. Wang, A cross-modality learning approach for vessel segmentation in retinal images, IEEE Trans. Med. Imaging 35 (1) (2016) 109–118.
[56] Z. Yao, Z. Zhang, L.-Q. Xu, Convolutional neural network for retinal blood vessel segmentation, in: Paper Presented at the Computational Intelligence and Design (ISCID), 2016 9th International Symposium on, 2016.
[57] A. Dasgupta, S. Singh, A fully convolutional neural network based structured prediction approach towards the retinal vessel segmentation, in: Paper Presented at the Biomedical Imaging (ISBI 2017), 2017 IEEE 14th International Symposium on, 2017.
[58] R. Welikala, P. Foster, P. Whincup, A. Rudnicka, C. Owen, D. Strachan, S. Barman, Automated arteriole and venule classification using deep learning for retinal images from the UK Biobank cohort, Comput. Biol. Med. (2017).
[59] X. Xu, T. Tan, F. Xu, An improved U-net architecture for simultaneous arteriole and venule segmentation in fundus image, in: Paper presented at the Annual Conference on Medical Image Understanding and Analysis, 2018.
[60] D. Maji, A. Santara, S. Ghosh, D. Sheet, P. Mitra, Deep neural network and random forest hybrid architecture for learning to detect retinal vessels in fundus images, in: Paper Presented at the Engineering in Medicine and Biology Society (EMBC), 2015 37th Annual International Conference of the IEEE, 2015.
[61] A. Lahiri, A.G. Roy, D. Sheet, P.K. Biswas, Deep neural ensemble for retinal vessel segmentation in fundus images towards achieving label-free angiography, in: Paper presented at the Engineering in Medicine and Biology Society (EMBC), 2016 IEEE 38th Annual International Conference of the, 2016.
[62] P. Prentašić, S. Lončarić, Detection of exudates in fundus photographs using deep neural networks and anatomical landmark detection fusion, Comput. Methods Programs Biomed. 137 (2016) 281–292.
[63] S. Abbasi-Sureshjani, B. Dashtbozorg, B.M. ter Haar Romeny, F. Fleuret, Boosted exudate segmentation in retinal images using residual nets, in: Fetal, Infant and Ophthalmic Medical Image Analysis, Springer, 2017, pp. 210–218.
[64] V. Gulshan, L. Peng, M. Coram, M.C. Stumpe, D. Wu, A. Narayanaswamy, et al., Development and validation of a deep learning algorithm for detection of diabetic retinopathy in retinal fundus photographs, JAMA 316 (22) (2016) 2402–2410.
[65] K.-K. Maninis, J. Pont-Tuset, P. Arbeláez, L. Van Gool, Deep retinal image understanding, in: Paper Presented at the International Conference on Medical Image Computing and Computer-Assisted Intervention, 2016.
[66] J.H. Tan, U.R. Acharya, S.V. Bhandary, K.C. Chua, S. Sivaprasad, Segmentation of optic disc, fovea and retinal vasculature using a single convolutional neural network, J. Comput. Sci. (2017).
[67] J. Zilly, J.M. Buhmann, D. Mahapatra, Glaucoma detection using entropy sampling and ensemble learning for automatic optic cup and disc segmentation, Comput. Med. Imaging Graph. 55 (2017) 28–41.
[68] J.H. Tan, H. Fujita, S. Sivaprasad, S.V. Bhandary, A.K. Rao, K.C. Chua, U.R. Acharya, Automated segmentation of exudates, haemorrhages, microaneurysms using single convolutional neural network, Inform. Sci. 420 (2017) 66–76.
[69] C. Lam, C. Yu, L. Huang, D. Rubin, Retinal lesion detection with deep learning using image patches, Invest. Ophthalmol. Vis. Sci. 59 (1) (2018) 590–596.
[70] M. Badar, M. Shahzad, M. Fraz, Simultaneous segmentation of multiple retinal pathologies using fully convolutional deep neural network, in: Paper Presented at the Annual Conference on Medical Image Understanding and Analysis, 2018.
[71] H. Pratt, F. Coenen, D.M. Broadbent, S.P. Harding, Y. Zheng, Convolutional neural networks for diabetic retinopathy, Procedia Comput. Sci. 90 (2016) 200–205.
[72] M.D. Abràmoff, Y. Lou, A. Erginay, W. Clarida, R. Amelon, J.C. Folk, M. Niemeijer, Improved automated detection of diabetic retinopathy on a publicly available dataset through integration of deep learningdeep learning detection of diabetic retinopathy, Invest. Ophthalmol. Vis. Sci. 57 (13) (2016) 5200–5206.
[73] E. Colas, A. Besse, A. Orgogozo, B. Schmauch, N. Meric, E. Besse, Deep learning approach for diabetic retinopathy screening, Acta Ophthalmol. 94 (S256) (2016).
[74] R. Gargeya, T. Leng, Automated identification of diabetic retinopathy using deep learning, Ophthalmology (2017).
[75] D.E. Worrall, C.M. Wilson, G.J. Brostow, Automated retinopathy of prematurity case detection with convolutional neural networks, in: Deep Learning and Data Labeling for Medical Applications, Springer, 2016, pp. 68–76.
[76] P. Burlina, D.E. Freund, N. Joshi, Y. Wolfson, N.M. Bressler, Detection of age-related macular degeneration via deep learning, in: Paper Presented at the Biomedical Imaging (ISBI), 2016 IEEE 13th International Symposium on, 2016.
[77] P. Burlina, K.D. Pacheco, N. Joshi, D.E. Freund, N.M. Bressler, Comparing humans and deep learning performance for grading AMD: A study in using universal deep features and transfer learning for automated AMD analysis, Comput. Biol. Med. 82 (2017) 80–86.
[78] C.S. Lee, D.M. Baughman, A.Y. Lee, Deep learning is effective for classifying normal versus age-related macular degeneration optical coherence tomography images, Ophthalmol. Retin. (2017) http://dx.doi.org/10.1016/j.oret.2016.12.009.
[79] J.Y. Choi, T.K. Yoo, J.G. Seo, J. Kwak, T.T. Um, T.H. Rim, Multi-categorical deep learning neural network to classify retinal images: A pilot study employing small database, PLoS One 12 (11) (2017) e0187336.

[80] S. Xie, Z. Tu, Holistically-nested edge detection, in: Paper Presented at the Proceedings of the IEEE International Conference on Computer Vision, 2015.
[81] T. Walter, J.-C. Klein, Segmentation of color fundus images of the human retina: Detection of the optic disc and the vascular tree using morphological techniques, in: Paper Presented at the International Symposium on Medical Data Analysis, 2001.
[82] A.F. Frangi, W.J. Niessen, K.L. Vincken, M.A. Viergever, Multiscale vessel enhancement filtering, in: Paper Presented at the International Conference on Medical Image Computing and Computer-Assisted Intervention, 1998.
[83] P. Costa, A. Campilho, Convolutional bag of words for diabetic retinopathy detection from eye fundus images, IPSJ Trans. Comput. Vis. Appl. 9 (1) (2017) 10, http://dx.doi.org/10.1186/s41074-017-0023-6.
[84] S. Otálora, O. Perdomo, F. González, H. Müller, Training deep convolutional neural networks with active learning for exudate classification in eye fundus images, in: Intravascular Imaging and Computer Assisted Stenting, and Large-Scale Annotation of Biomedical Data and Expert Label Synthesis, Springer, 2017, pp. 146–154.
[85] Y. Nesterov, A method for unconstrained convex minimization problem with the rate of convergence O (1/k^2), in: Paper Presented at the Doklady AN USSR, 1983.
[86] X. Glorot, Y. Bengio, Understanding the difficulty of training deep feedforward neural networks, in: Paper Presented at the Proceedings of the Thirteenth International Conference on Artificial Intelligence and Statistics, 2010.
[87] J. Sivaswamy, S. Krishnadas, G.D. Joshi, M. Jain, A.U.S. Tabish, Drishti-gs: Retinal image dataset for optic nerve head (onh) segmentation, in: Paper Presented at the 2014 IEEE 11th International Symposium on Biomedical Imaging (ISBI), 2014.
[88] V. Badrinarayanan, A. Kendall, R. Cipolla, Segnet: A deep convolutional encoder–decoder architecture for image segmentation, IEEE Trans. Pattern Anal. Mach. Intell. 39 (12) (2017) 2481–2495.
[89] C. Szegedy, V. Vanhoucke, S. Ioffe, J. Shlens, Z. Wojna, Rethinking the inception architecture for computer vision, in: Paper Presented at the Proceedings of the IEEE Conference on Computer Vision and Pattern Recognition, 2016.
[90] G. Dahl, A.-r. Mohamed, G.E. Hinton, Phone recognition with the mean-covariance restricted Boltzmann machine, in: Paper Presented at the Advances in Neural Information Processing Systems, 2010.
[91] P. Prentašić, S. Lončarić, Detection of exudates in fundus photographs using convolutional neural networks, in: Paper presented at the Image and Signal Processing and Analysis (ISPA), 2015 9th International Symposium on, 2015.
[92] J. Shan, L. Li, A deep learning method for microaneurysm detection in fundus images, in: Paper presented at the Connected Health: Applications, Systems and Engineering Technologies (CHASE), 2016 IEEE First International Conference on, 2016.